

August 1, 2005

Ken Zweibel  
National Renewable Energy Laboratory  
1617 Cole Boulevard  
Golden, CO 80401

Re: NREL Subcontract #ADJ-1-30630-12

Dear Ken:

This report covers research conducted at the Institute of Energy Conversion (IEC) for the period of June 9, 2005 to July 9, 2005, under the subject subcontract. The report highlights progress and results obtained under Task 1 (CdTe-based Solar Cells).

### **Task 1 – CdTe-based Solar Cells**

Different aspects of processing vapor transport (VT) solar cells were evaluated and new processing options to address key issues of high throughput are being developed. In particular, variations in device performance are correlated with systematic variations in the CdCl<sub>2</sub> treatment and with the exposure of fresh CdTe surfaces to humid ambient prior to CdCl<sub>2</sub> treatment. With respect to CdTe deposition, characterization of the VT deposition system was carried out to refine the quantitative model used to monitor deposition rate and Cd utilization. With respect to surface treatments for back contact processing; alternatives to BDH processing, such as aniline treatment, continue to be investigated. Temperature dependant bifacial QE measurements gave new insights into the CdTe device physics. The formation rate and composition of oxide phases in CdTe films was investigated with respect to humidity. Participation in the National CdTe R&D Team meeting held in May 2005 is described.

### ***Baseline CdTe Cell Processing***

Considerable variability in cell performance for nominally identically processed VT runs has been experienced during the later spring and early summer. It has been well established that repeatability and high efficiency are difficult to achieve for batch processing in the humid summer months, since both the CdTe surface and CdCl<sub>2</sub> source powder are sensitive to humidity.

At the May 2005 National CdTe R&D Team Meeting, Brian McCandless showed how device performance is reduced by exposure of the CdTe/CdS films to humidity prior to CdCl<sub>2</sub> treatment. Figure 1 shows the J-V characteristics for three cells fabricated from the same VT CdTe/CdS plate but exposed to different ambient prior to CdCl<sub>2</sub> treatment. The J-V parameters are listed in Table I. The sample kept in vacuum from deposition until CdCl<sub>2</sub> treatment attained 12% efficiency. Storing a sample at 40°C overnight, in humid air, resulted in a decrease in all cell

parameters, but primarily affected  $V_{OC}$  and FF. This trend continued for the sample exposed to humid air for a few minutes at 400°C, marked by an increase in series resistance sufficient to affect  $J_{SC}$ . Glancing incidence x-ray diffraction (GIXRD) measurements of the surface of physical vapor deposition (PVD) and VT CdTe films stored in humid ambient, often exhibit reflections due to  $CdTe_2O_5$ , which forms by selective oxidation of Te with oxygen. In dry ambient no detectable oxides form, unless the samples are heated above 250°C, in which case  $CdTeO_3$  is formed, by stoichiometric reaction of CdTe with oxygen. It is believed that the desired defects needed for high efficiency CdTe/CdS cells are only formed for CdTe films, in which the Cd-Te stoichiometry has not been appreciably altered prior to  $CdCl_2$  processing. Collaboration with the group at Colorado State University is proceeding to determine defects using photoluminescence measurements of PVD and VT CdTe films under different sample preparation conditions.

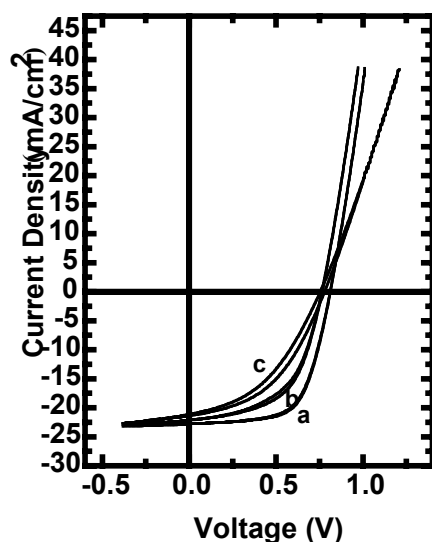


**Figure 1. Light J-V plots for three devices made from the same VT CdTe/CdS plate but exposed to different levels of humidity prior to  $CdCl_2$  treatment: a) stored in vacuum for 1 week; b) stored in humid room air,  $[H_2O] \sim 0.1$  g/L, at 40°C for 16 hours; c) heated in humid air,  $[H_2O] \sim 5$  g/L at 400°C for 5 min.**

**Table I. J-V parameters for the cells of Figure 1.**

Sample	Condition prior to vapor $CdCl_2$	$V_{OC}$ (mV)	$J_{SC}$ ( $mA/cm^2$ )	FF (%)	Eff (%)
161.2 (a)	Vacuum Stored 25°C, 1 week	812	23	64	12.0
161.2 (b)	Stored in air 40°C, 16 hr 9~0.1 g/L)	764	22.5	56	9.5
161.4 (c)	HT in air 400°C 5 min (5 g/L)	778	22	45	7.5

The  $\text{CdCl}_2$  step is also sensitive to ambient, and the source itself can evolve over time. For the baseline treatment used at IEC, the  $\text{CdS}/\text{CdTe}$  structures are exposed to  $\text{CdCl}_2$  in a reactor configured in close-space sublimation mode, in which the  $\text{CdCl}_2$  source powder is pressed into a graphite susceptor parallel to the  $\text{CdTe}$  specimen, which is held on a mica spacer  $\sim 1$  mm from the  $\text{CdCl}_2$  surface. Both the substrates and the  $\text{CdCl}_2$  are radiatively heated by quartz FCM type lamps. Typically, isothermal reactions are carried out with both substrate and  $\text{CdCl}_2$  temperature equal to  $420^\circ\text{C}$ . The system is maintained under flowing argon and is operated with a bake at  $200^\circ\text{C}$  under vacuum before each sample is treated. These steps are crucial in spring and summer, when ambient humidity is high. In a previous report, we showed how the chemical composition of the  $\text{CdCl}_2$  powder changes, with exposure to humid ambient, resulting in the formation of cadmium chlorates.<sup>1</sup> Without properly dessicating the source and sample before each treatment, the close-space treatment configuration entraps the liberated water, whereupon it becomes a reactive species in the vapor ambient.

During this year, the same  $\text{CdCl}_2$  source has been used and recently, device performance suggested insufficient  $\text{CdCl}_2$  exposure despite identical  $\text{CdCl}_2$  treatments. Visual inspection of the  $\text{CdCl}_2$  bed, after removing from the susceptor, indicated that the  $\text{CdCl}_2$  powder had fused into mm-size platelets at the  $\text{CdCl}_2$ -susceptor interface. This change would reduce the total  $\text{CdCl}_2$  surface area and reduce the heat transfer from the susceptor, both of which would significantly reduce the  $\text{CdCl}_2$  evaporation rate. This was verified by performing  $\text{CdCl}_2$  depositions onto glass substrates, resulting in significantly thinner deposits than obtained with a fresh source. A fresh  $\text{CdCl}_2$  source bed was prepared, and pieces from four identically deposited  $\text{CdCl}_2$  “baseline” runs were treated (VT170, 172, 173, 174). The pieces came from the same location of the  $\text{CdS}/\text{CdTe}$  plate to eliminate possible spatial variations in the VT reactor. They were given the  $\text{CdCl}_2$  treatment (20 min in  $\text{Ar}/\text{O}_2$  at  $420^\circ\text{C}$ ) in a random order to eliminate any sequential degradation in the VT system. After  $\text{CdCl}_2$  treatment, they were all processed identically, receiving BDH etching and 15 nm Cu/ 50 nm Ni contacts in the same evaporator run. There were 8 cells per piece with  $0.36\text{ cm}^2$  area.

The device results are shown in Figure 2. The x-axis is their sequence in the  $\text{CdCl}_2$  process after replacing the source. Data is shown for both best cell per piece and average, after eliminating obviously shunted devices ( $\text{FF} < 40\%$  or  $G_{\text{sc}} > 15\text{ mS}/\text{cm}^2$ ). The best device was VT174.1-3, the first piece to receive  $\text{CdCl}_2$  treatment, and had  $V_{\text{OC}} = 0.793\text{ V}$ ,  $J_{\text{SC}} = 23.4\text{ mA}/\text{cm}^2$ ,  $\text{FF} = 69.9\%$  and  $\text{efficiency} = 12.9\%$ , consistent with our typical best cell performance. However, the average values and the best single cell values degrade significantly after 1 or 2  $\text{CdCl}_2$  treatments. The average  $V_{\text{OC}}$  decreased  $0.1\text{ V}$  and the average  $\text{FF}$  by 10 points. The yield is also shown in the bottom graph of Figure 2. Looking from the first to the fourth piece in the sequence, average efficiency decreased from 11.0 to 7.0% and the yield decreased from 87 to 50%. The hysteresis, determined from difference in maximum power between the up and down J-V traces also increased significantly from the first to fourth piece. Thus, all measurable device parameters degraded with subsequent processing with the same  $\text{CdCl}_2$  source. Re-compacting the source into the susceptor base restores  $\text{CdCl}_2$  delivery as shown by depositions onto glass, resulting in recovery of cell performance. However, re-packing the bed or otherwise preparing a fresh  $\text{CdCl}_2$  source bed for each treatment is impractical and unreliable, and new methods are being developed for reproducibly delivering both  $\text{CdCl}_2$  vapor and  $\text{O}_2$  to the  $\text{CdTe}$  surface. Results will be presented in the next report.

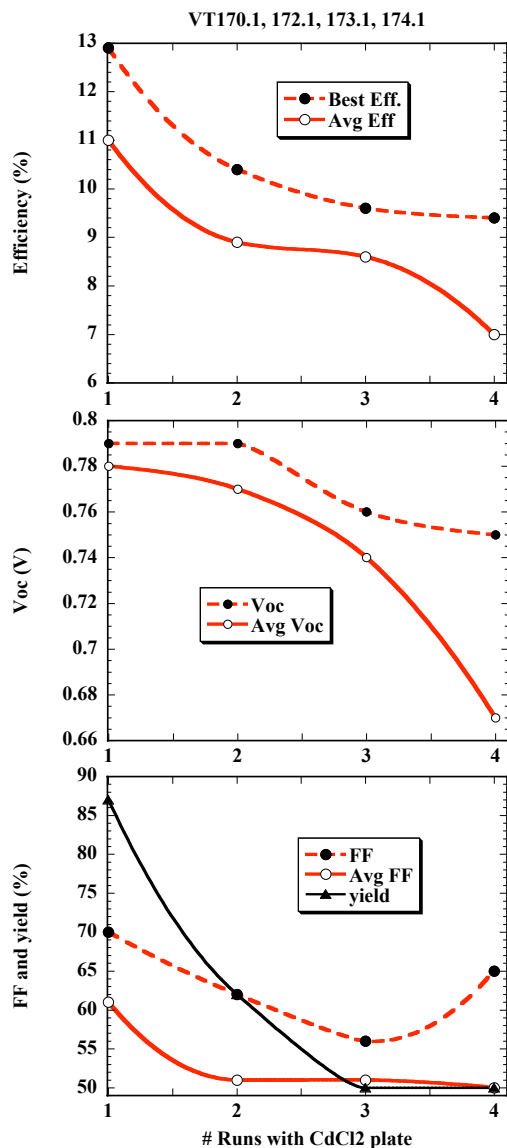


**Figure 2. The Eff,  $V_{OC}$ , FF and yield versus the sequence in  $CdCl_2$  processing. Both best cell and averaged values are shown. Yield is defined in text.**

Experiments with humid ambient exposure, described above, demonstrate that the “starting point” of the CdTe/CdS structure can strongly influence the obtained cell performance. To examine the variation from the CdTe and CdS depositions themselves in more detail, contacts were evaporated onto raw CdTe/CdS plates without receiving any  $CdCl_2$  treatment. The CdTe and CdS films were 5-8 microns and 80 nm thick, respectively, and were stored in a dry box prior to contacting. Contact was made by sequential evaporation of 15 nm Cu and 50 nm Ni.

Cells were heated in argon at 180°C for 20 min and briefly etched in weak  $\text{Br}_2:\text{CH}_3\text{OH}$  to clean the surface. The J-V parameters of the best cells on each piece are listed in Table II.

**Table II. J-V parameters for cells made with no  $\text{CdCl}_2$  treatment and no etching prior to contacting.**

Sample	Thickness ( $\mu\text{m}$ )	Storage Time (days)	$V_{\text{OC}}$ (mV)	$J_{\text{SC}}$ ( $\text{mA}/\text{cm}^2$ )	FF (%)	Eff (%)	$R_{\text{OC}}$ ( $\Omega/\text{cm}^2$ )
148.4	7.2	106	610	8.1	53	2.6	16
149.6	6.9	106	620	7.2	53	2.4	18
154.5	7.6	50	545	2.9	43	0.7	51
167.6	5.4	14	630	9.4	52	3.1	15

The statistical spread of cell performance was less than 10 rel% on all four samples. Three of the samples show comparable performance, and one sample exhibits markedly lower performance and higher series resistance than the others, neither film thickness nor time in storage account for the deviation. The efficiencies of the best cells obtained from each plate, using  $\text{CdCl}_2$  and surface treatment with Cu/Ni contacts, are not correlated with those of the untreated samples: VT148 Eff = 8.3%; VT149 Eff = 11.5%; VT154 Eff = 11.5%; and VT 167 Eff = 11.1%. The efficiencies in Table II are much higher than we would have obtained from PVD CdTe devices, without  $\text{CdCl}_2$  treatment, indicating that the VT material is much closer to optimum as-deposited.

## Vapor Transport Deposition

Calibration measurements of the temperature within the CdTe source of the VT deposition system were carried out, to provide the data needed to quantitatively compare the measured source output and growth rate, with those predicted by a model of the deposition system. The analytic model for the VT source, which led to the design and construction of the VT system, has been refined and compared to a finite element model. The accuracy of the analytic model has been validated by comparison with the measured data for a wide range of conditions. The approach can be extended for use with other congruently subliming materials by consideration of their saturation pressure and diffusivity in the carrier gas. A manuscript, "Design Methodology of a Vapor Transport Deposition Process," has been written for submission.

### *Temperature dependent bifacial spectral response*

Transparent ZnTe: Cu contact based CdTe cells have been successfully developed at IEC. These cells have demonstrated  $V_{\text{OC}}$ , FF and efficiencies comparable to the cells with the same absorber material, but different back contacts materials like Cu/Ni and Cu/Au. These cells, with transparent (semi) back contact, have the added advantage of being a useful bifacial junction characterization tool. We have investigated the properties of CdS/CdTe junctions at low

temperature using this device.  $J_{SC}$  was measured at different light intensities in the temperature range of 100-300K for front and back illumination and the effective QE was determined.

Figure 3 shows the  $J_{SC}$  measured for two different light intensities for illumination through front contact ( $\text{SnO}_2/\text{CdS}$ ) and back contact ( $\text{ITO}/\text{ZnTe}:\text{Cu}$ ).  $J_{SC}$  for front illumination decreases slightly within temperature range 200-300K and then rapidly decreases below 200K. Opposite behavior is observed for back illumination. The  $J_{SC}$  increases when the temperature is lowered. In the previous report, we mentioned the behavior of  $V_{OC}$  as a function of temperature. Typically, all the cells studied to date show  $V_{OC}$  saturation and negligible intensity dependence for temperatures below 200K. CdTe cells have a large depletion region, even at room temperature, which ensures efficient carrier collection. The  $J_{SC}$  for front and back illumination shows opposite temperature dependence.

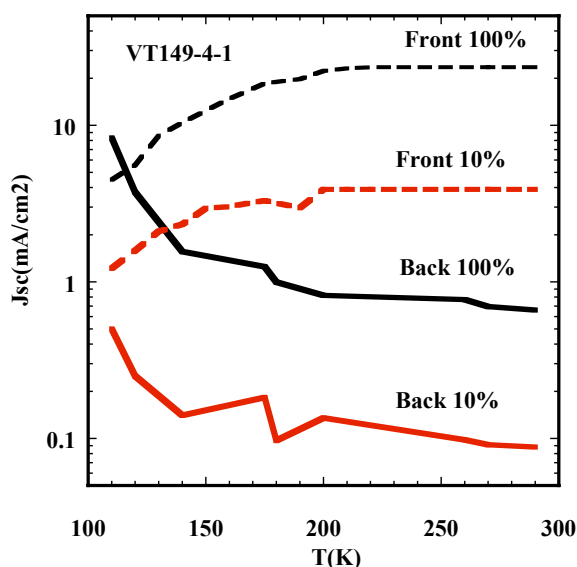


**Figure 3.  $J_{SC}$  as a function of temperature for front and back illumination at 100 and 10% intensity. Note the log scale.**

The  $J_{SC}$  for these cells was measured as a function of temperature using narrow band pass filters having FWHM~25 nm. The correction factors for filter transmission and the ELH lamp spectrum were determined using the QE, as measured on our standard monochromator based chopped light QE system at 300K, as a reference. The QE as a function of temperature was then calculated from the  $J_{SC}$  values. Figures 4 and 5 show the QE calculated for the front and back illumination for different temperatures.

Due to the high absorption coefficient, most of the carriers generated for front illumination are efficiently collected in the high field region located near CdS/CdTe interface. For the back illumination, the carrier-collection is limited by diffusion length of the carriers to that front junction. Only the carriers generated close enough to diffuse to the collecting junction can contribute to the photocurrent ( $J_{SC}$ ). This has been discussed and modeled in previous reports.

Applying this model to interpret, Figure 5 indicates that the diffusion length and depletion region increase with decreasing temperature.

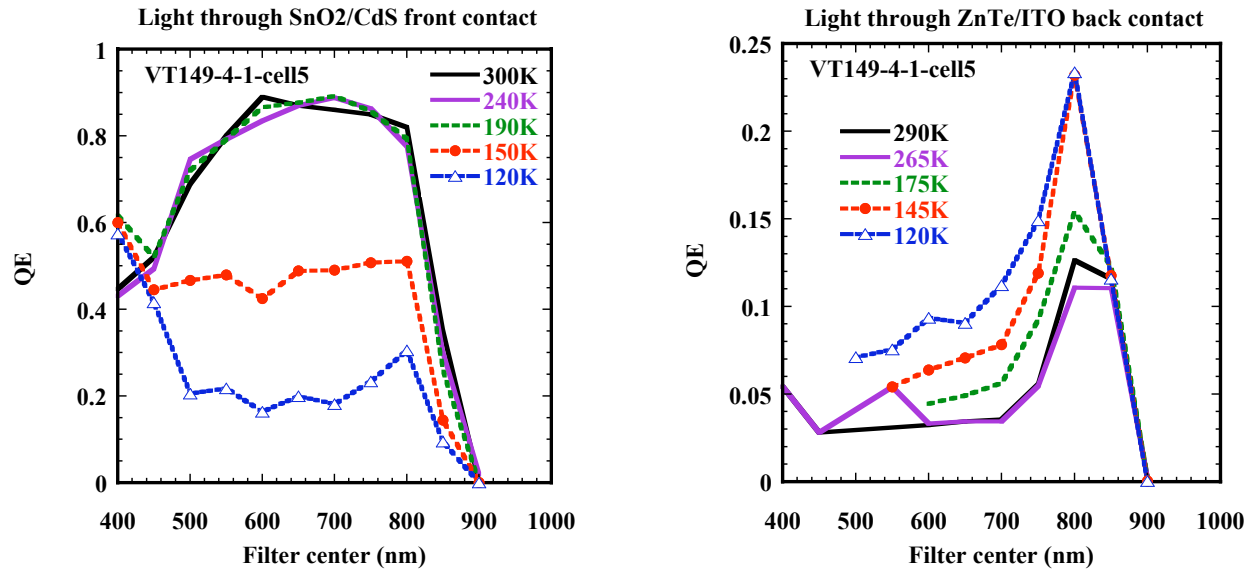


**Figure 4.(Left) QE as calculated from  $J_{SC}$  measured using filters for front illumination.**  
**Figure 5.(Right) QE as calculated from  $J_{SC}$  measured using filters for back illumination.**

We intend to measure the CV response to obtain an independent confirmation of the depletion width. We also plan to measure cells with thinner absorber layers. Work has begun on a manuscript, describing our understanding of CdTe device physics, based on characterization with front and back illumination.

### ***Contact Processing: Aniline Etching of CdTe***

Testing of the aniline treatment of CdTe, in collaboration with the University of Toledo, has continued. Treatment of CdTe in aniline-based aqueous solutions, with illumination, generates a uniform crystalline Te-rich surface layer, suitable for back contact processing of devices. Optimization has found that best results are obtained from aqueous baths containing 0.1 M aniline (structure in Figure 6a), 0.01 M p-toluenesulfonic acid (p-TSA) and 1 M NaCl. In the previous report, a series of results was presented for devices etched for varying times. In that case, 30 min treatments with illumination directly on the CdTe film, and 60 min treatments with illumination on the glass side of the sample, both produced the best devices, indicating these two treatments produced similar surfaces. Longer treatments, with illumination directly on the CdTe film, produced poorer devices, possibly due to grain boundary etching. Further investigations of the treatment times on device performance have been carried out, comparing shorter treatment times for illumination on the CdTe and longer times for illumination of the glass.

Bath conditions were as described above. Samples consisted of vapor-CdCl<sub>2</sub> treated ~5  $\mu$ m thick CdTe films VT deposited on SnO<sub>2</sub>/glass coated with ~50 nm chemical solution deposited CdS

films. Devices were processed, following aniline treatment times of 5, 10, 20 and 30 min with light on the CdTe and 60, 120 and 180 min with light on the glass, by applying a Cu-based back contact, completing with a graphite paste secondary contact and annealing for 15 min at 200°C in Ar(g). Device results showed, for illumination directly on CdTe, the best devices were obtained following 30 min treatment. Devices processed with treatment times <30 min exhibited poorer  $J_{SC}$  and fill factor and increased series resistance. This suggests these devices have poorer back contacts, due to incomplete etching of the CdTe surface. Longer treatment times, >60 min, with illumination on the glass, also resulted in decreased device performance, likely due to grain boundary etching. We confirm that the best aniline-treated devices are obtained with 30 min treatments, with illumination on the CdTe, or with 60 min treatments with light on the glass.

Due to its toxicity, we are seeking safer substitutes for aniline. We have previously reported a number of criteria for possible substitutes, including oxidation potentials similar to aniline and oxidation products that are non-reactive towards CdTe and Te. Preliminary experiments have highlighted 8-hydroxyquinoline (8-HQ, Figure 6b) and 1-naphthylamine (1-NA, Figure 6c) as potential replacements. Both of these species are significantly less toxic than aniline and 1-NA has a similar oxidation potential to aniline and polymerizes when oxidized.<sup>2</sup> Treatment of CdTe with illumination in saturated solutions of 8-HQ and 1-NA, containing p-TSA and NaCl, both resulted in the formation of uniform Te-rich layers. 1-NA solutions showed no reaction with CdTe when treated in the dark; however, dark treatments in 8-HQ resulted in weak etching of the film, likely due to stripping of surface  $Cd^{2+}$  ions by complexation. Investigations of the suitability of these species for CdTe device processing will continue.

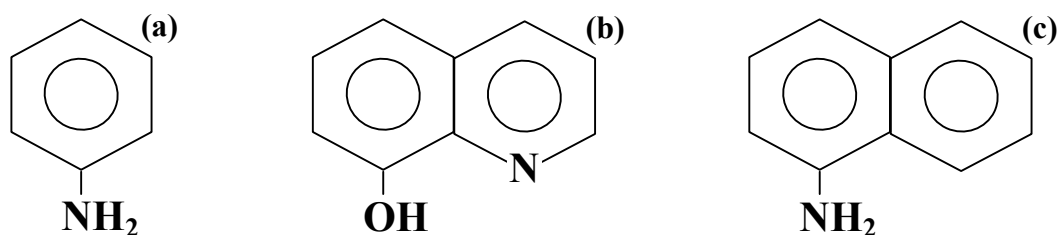


**Figure 6. Structure of (a) aniline, (b) 8-hydroxyquinoline and (c) 1-naphthylamine.**

### ***CdTe Oxidation***

The oxygen used to process CdTe/CdS solar cells reacts with, and is incorporated into, the film structure. Native oxidation can lead to  $CdTeO_3$  or  $CdTe_2O_5$ , depending on the conditions of the oxidation, and the various oxidation routes are not yet determined. During  $CdCl_2$  treatment, reaction between CdTe and  $CdCl_2$  produces CdO, as an oxide residue, and  $TeCl_2$  as a vapor product. On cells which have significant oxide accumulation, etching is required to facilitate contact formation. However, the various etches do not always completely remove penetrating oxides, and completed solar cells with efficiencies of 11%, such as PVD cells made at IEC and electrodeposited cells, formerly made by BP Solar, can contain measurable quantities of the



oxides CdO and CdTeO<sub>3</sub>. A key question is centered on the idea that if the oxides populate the grain boundaries and are benign for cell performance, do they affect transport of other impurity species, which may affect stability. The question may apply to all CdTe cells, since the oxides may exist at concentrations below the detection limit of methods such as XRD, EDS, or XPS.

Experiments have been conducted to form native oxides on PVD CdTe films under conditions of different humidity, at  $[\text{H}_2\text{O}] < 0.001 \text{ g/L}$ ,  $[\text{H}_2\text{O}] < 0.05 \text{ g/L}$ , and  $[\text{H}_2\text{O}] \sim 0.1 \text{ g/L}$ . PVD films deposited at 300°C were selected for the initial experiments because of inherent specimen flatness. GIXRD with an in-situ heating stage was used to measure the crystalline phases formed, and XPS depth profile measurements were carried out afterwards to probe the oxide-telluride interfacial region. Figure 7 shows GIXRD results for treatment at 500°C in dry air,  $[\text{H}_2\text{O}] < 0.001 \text{ g/L}$ , and in humid air,  $[\text{H}_2\text{O}] \sim 0.1 \text{ g/L}$ . In both cases, the CdTe (111) peak intensity decreases while oxide peaks increase with increasing treatment time. For dry air, only one oxide,  $\alpha\text{-CdTeO}_3$  (monoclinic) is detected. For humid air, an initial TeO<sub>2</sub> phase is detected but then transitions to a mixture of  $\alpha\text{-CdTeO}_3$  and  $\beta\text{-CdTeO}_3$ . The rate of oxidation can be estimated from the GIXRD measurements by both the rate of decrease in CdTe (111) intensity and by the accumulation rate of oxide peaks. Both methods indicate that the humid treatment initially increases the oxidation rate by >10X and that the oxidation then becomes diffusion limited. The oxides, which form in the short time interval, are being investigated to determine the chemical path for oxide formation under different humidity levels.

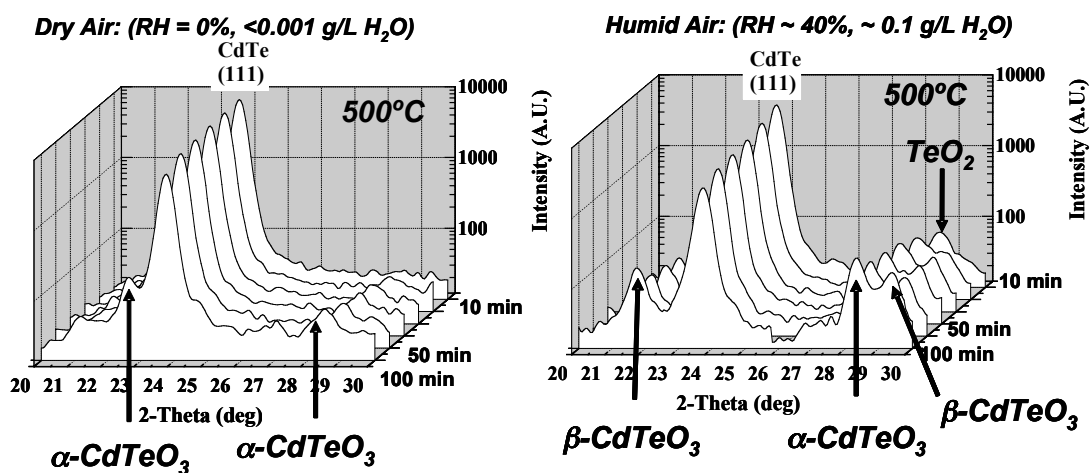


**Figure 7. Time-progressive GIXRD scans of PVD CdTe films oxidized at 500°C in dry and humid ambient.**

X-ray photoelectron spectroscopic (XPS) depth profiles using Al K $\alpha$  radiation indicate that in addition to a surface oxide, a penetrating oxide is present (Figure 8). For both specimens there is a gradual transition from Te-O to Te-Cd bonding with sputter depth, with enhanced oxidation for the sample treated in humid air.

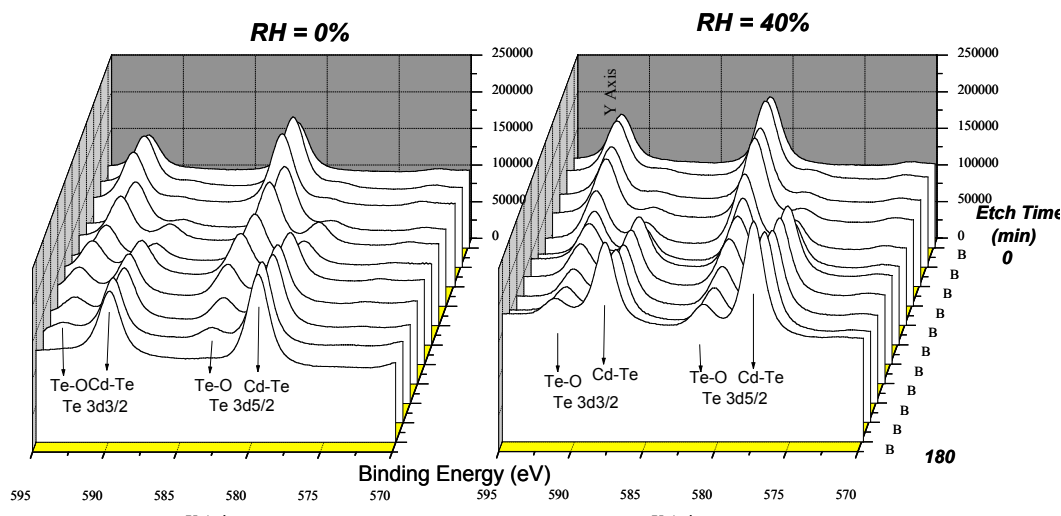


Figure 8. XPS depth profiles of the films of Figure 7, using Al K $\alpha$  radiation.

The properties of CdTeO<sub>3</sub> are not well investigated. Therefore a film was synthesized by oxidation of a PVD CdTe film on Corning 7059 glass in dry air for a period of 400 hours at 600°C. The XRD pattern of the resulting film contained only peaks of b-CdTeO<sub>3</sub>, corresponding to the crystallographic data of Wroblewska<sup>3</sup> with symmetry P2<sub>1</sub>/c (space group 14). The optical transmission was measured (Figure 9) and the absorption coefficient calculated. On a plot of  $\alpha^2$  versus energy, two linear regions are found, extrapolating to transition energies of 2.94 eV and 3.65 eV (Figure 10). The conductive properties of the film will be reported in the coming period.

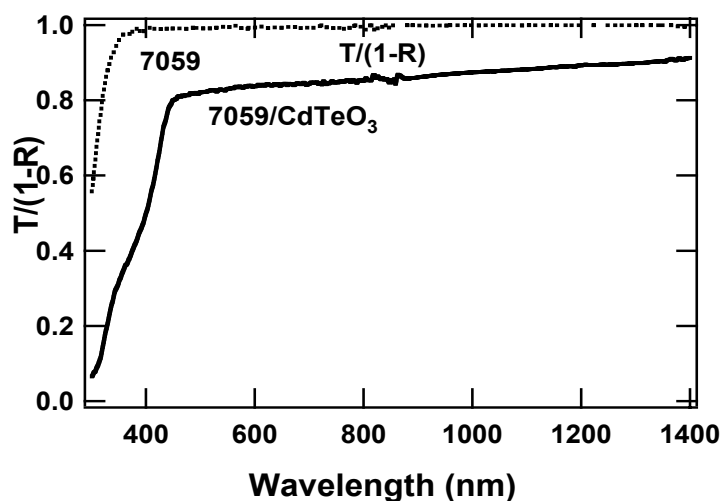
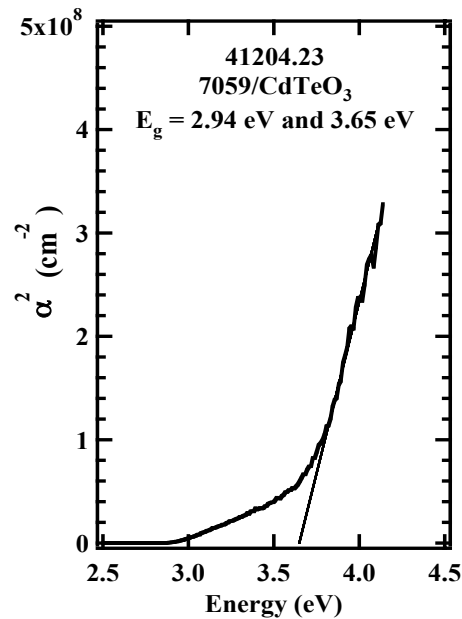


Figure 9.  $T/(1-R)$  versus wavelength of 1.5 mm thick CdTeO<sub>3</sub> film on Corning 7059 glass.



**Figure 10. Absorption coefficient versus energy of 1.5 mm thick CdTeO<sub>3</sub> film on Corning 7059 glass.**

#### **Team Activity and Collaboration:**

Steve Hegedus and Brian McCandless attended the CdTe National Team Meeting, held at NREL on May 5-6, 2005, and participated in the three sub-teams. Steve Hegedus presented work on bifacial solar cells and on the effects of bias application during cell stressing. Brian McCandless served as co-leader of the materials chemistry and analysis sub-team, and presented work on the sensitivity of device operation to processing chemistry. Collaborative work between IEC and other groups was also presented. Timothy Gessert visited IEC on June 7-8, 2005 to discuss VT deposition.

Best regards,

Robert W. Birkmire  
Director

RWB/bj

Cc: Brian McCandless  
Kevin Dobson  
Steven Hegedus  
Gerri Hobbs, UD Research Office  
Carolyn Lopez, NREL

## References

---

<sup>1</sup> IEC Monthly Report to NREL for Phase 2 of this contract, Aug 2003.

<sup>2</sup> H. Li, L. S. Less, D. G. Schulze and C. A. Guest, *Environ. Sci. Technol.*, **37** (2003) 2686.

<sup>3</sup> J. Wroblewska, *Rev. chim. Miner.* 16 (1979) 112.